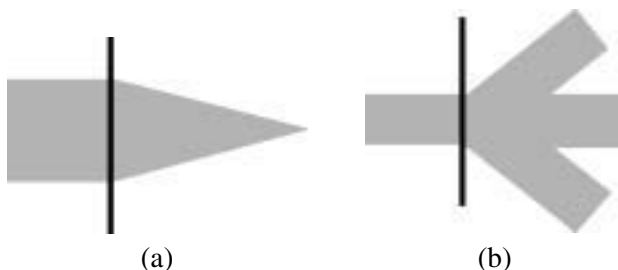


## Chapter 5

# Design of Diffraction Gratings

### 5.1 Introduction

The discussion in Chapter 4 centered on the design of diffractive optics using conventional lens design techniques, in which each ray incident on the DOE is mapped to one output ray. The refractive lenses and mirrors and the diffractive elements described in Chapter 4 manipulate the wavefront by a 1-to-1 mapping [Fig. 5.1(a)]. Diffractive structures can also be used by the optical engineer for wavefront splitting, in which elements are designed to send light into multiple diffraction orders [Fig. 5.1(b)]. In this chapter we discuss the characteristics and design techniques for diffractive optics that perform a 1-to- $N$  mapping. The techniques used to design complex gratings can be applied to more general classes of diffractive optics, but for consistency we illustrate these design approaches using gratings.



**Figure 5.1** Wavefront mapping. (a) 1-to-1 wavefront mapping—the diffractive element mimics a refractive lens. (b) 1-to-3 mapping—the diffractive element acts as a beam-splitting grating.

#### 5.1.1 Splitting a wavefront

When a beam of light passes through any periodic structure, it will be diffracted into multiple orders. The period of the repeated structure determines the angular separation between the orders. A small period creates large angular separation, while a large period results in closely spaced output beams. The angle  $\theta_m$  of each output beam of order  $m$  relative to the zero-order beam is given by the grating

equation:

$$\sin \theta_m = m\lambda/\Lambda, \quad (5.1)$$

where  $\Lambda$  is the period of the structure.

Although the grating equation determines *where* the light is directed, it does not determine the relative power directed into each of the diffracted orders. This power distribution is dictated by the shape and nature of the surface profile within a single grating period. As we saw in Chapter 2, if the shape within a unit cell of the periodic structure is an ideal blaze, all of the diffracted light is transmitted into the +1 order. An identical shape with a smaller phase depth will split light between the 0 and +1 orders, as well as diffracting smaller quantities into the other orders. The more complicated grating structures allow the wavefront to be split into essentially arbitrary power distributions between the output orders. A wide variety of phase structures, as well as attenuating or blocking features, can be incorporated into the unit cell of a periodic structure. The ability to harness this design freedom is a major benefit of diffractive optics. The creation of these special gratings and splitters requires an understanding of the design variables and, in all but the simplest of cases, a computer.

### 5.1.2 A 1 × 3 grating

A simple periodic structure, the binary phase grating, was introduced in Chapters 2 and 3. In Fig. 2.9, the binary phase grating was shown as a first approximation of a continuous-blazed grating. The binary approximation, however, is only 40.5% efficient in the +1 diffraction order. This binary profile is an equally good approximation of an ideal blaze in the opposite direction, so it follows that this grating is also 40.5% efficient in the −1 diffraction order. Thus, a linear binary grating with a fixed period can also be considered to be an 81% efficient beamsplitter or 1 × 2 grating (see Fig. 2.8). The remaining light is diffracted into higher orders.

To provide additional insight into the control of the various grating orders, we introduce an additional degree of freedom into our binary phase grating design: the duty cycle, which is the ratio of the feature dimension  $b$  to the period of the grating  $\Lambda$ . For the present, we will consider only binary gratings. Also, we will retain the same etch depth  $d$  that provides a half-wave optical path difference between the two grating levels.

To understand the binary phase grating, it is best to analyze it in the context of Fourier optics using the convolution theorem. From the physical definition of the grating, one can quickly create a mathematical description of the element using the convolution operation and the Dirac delta function, as discussed in Chapter 2. The mathematical description of the unit cell is two offset rect functions with a phase constant applied to the second one (Fig. 5.2). The offset is accomplished with the delta function.

$$\begin{aligned} \text{unit cell} = f(x) = & [\text{rect}(x/b) \otimes \delta(x + b/2)] \\ & + \{\text{rect}[x/(\Lambda - b)] \otimes \delta[x - (\Lambda - b)/2]\} e^{i\phi}. \end{aligned} \quad (5.2)$$

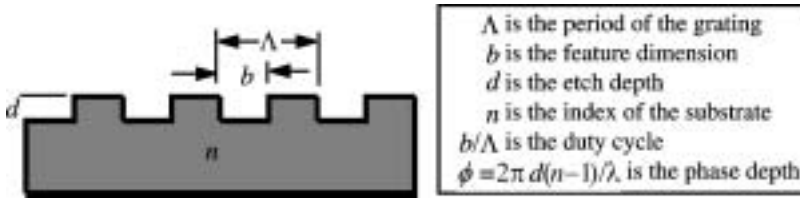


**Figure 5.2** The physical definitions of a binary phase grating.

Having defined the unit cell, an infinite grating can be generated with one additional convolution with the comb function:

$$\text{grating} = f(x) \otimes \text{comb}(x/\Lambda). \quad (5.3)$$

As discussed in Sec. 2.3, the discrete orders propagate at angles  $\theta_m$  given by the grating equation [Eqs. (2.26) and (5.1)]. Therefore the Fourier transform of the grating is only defined at discrete intervals, the orders of the grating, which correspond to the transform of  $\text{comb}(x/\Lambda)$ . The result of this Fourier transform is also a comb function:  $\text{comb}(\Lambda q)$ , which has a unit value at  $q = m/\Lambda$ , where  $m$  is any integer.

The Fourier transform of the unit cell,  $\mathfrak{F}[f(x)] = F(q)$ , forms an envelope function, the function that multiplies the comb function and gives the amplitude and relative phase of each diffracted order. As noted in Sec. 2.4.1, the Fourier transform of the  $\text{rect}(x)$  function is  $\text{sinc}(q)$ . Therefore, the transform of  $f(x)$ , which describes the unit cell, is the sum of two sinc functions with offset phase terms.

$$F(q) = \frac{b}{\Lambda} \frac{\sin(\pi b q)}{\pi b q} \exp(i2\pi q b/2) + \frac{(\Lambda - b)}{\Lambda} \frac{\sin[\pi(\Lambda - b)q]}{\pi(\Lambda - b)q} \exp[i2\pi q(\Lambda - b)/2]. \quad (5.4)$$

In the case of our earlier binary phase grating, where  $b = \Lambda/2$  and  $\phi = \pi$ , this simplifies to

$$F(q) = \frac{1}{2} \frac{\sin(\pi b q)}{\pi b q} [\exp(i\pi b q) - \exp(-i\pi b q)]. \quad (5.5)$$

Restating this envelope function for the values where the comb function is nonzero, the output of the grating is given by

$$|F(q)|_{q=m/\Lambda} = \frac{\sin(m\pi/2)}{m\pi/2} [i \sin(m\pi/2)], \quad (5.6)$$

## Chapter 6

# Making a Diffractive Optical Element

In previous chapters we considered the fundamental theories of diffraction and a number of design approaches for diffractive optical elements. However, before a diffractive optical element can be built, a number of additional questions must be addressed. For example:

- How is the design in a computer “transformed” into a physical component?
- What material should the DOE be made from?
- How does the choice of material affect the fabrication process?
- Are there physical limitations on what can be made?
- How does the quality of the substrate affect the performance of the components?
- Are special pieces of equipment or special environments required for the fabrication process?
- How do you know what you have made?

These topics will be explored in detail in the next several chapters. In general, we will explore the manufacture and test of spatially varying phase profiles in or on an optical substrate. Although this phase profile can be achieved through a number of means, the most common realization of these profiles will be considered: Diffractive optical elements created as spatially varying surface relief profiles in or on an optical substrate.

### 6.1 The Profile

The surface relief profiles of diffractive elements can take on a wide range of shapes that depend on the optical function of the component. Consider the simple binary phase structure that was analyzed in Chapter 5 and is shown in Fig. 6.1. When the depth  $d$  is equal to a half-wave optical path difference (discussed later) and the duty cycle,  $b/\Lambda = 1/2$ , the grating is a square-wave type. This grating will split a normally incident light beam, with approximately 81% of the transmitted

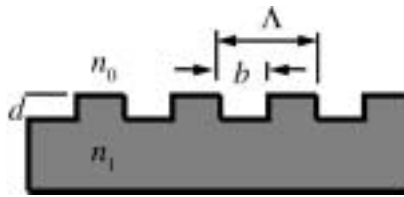


**Figure 6.1** Geometry of a simple binary phase diffractive element.

light split equally between the positive first and negative first diffraction orders, as discussed in Sec. 2.4.1. As more elaborate and efficient diffractive structures are required, the complexity of the surface structure increases rapidly. Depending on the desired optical functionality, the required surface patterns might have two-phase steps, multiple-phase steps, or even be essentially continuous-relief surface profiles. Lateral patterns can be one or two dimensional, with varying degrees of symmetry or asymmetry. Submicron precision may be required for feature widths, and depth tolerances on the order of 10 nm or less may be needed. Simply stated, the fundamental problem in DOE manufacturing is: How do you fabricate these microscopic surface relief structures with the correct geometries?

Many different methods exist for fabrication of diffractive microstructures.<sup>1</sup> Most of these techniques can be grouped into three main categories: lithographic techniques, direct machining, and replication. Lithographic techniques (originally developed in the microelectronics industry) use light-sensitive polymers in conjunction with controlled etching or deposition methods. In direct machining, the surface relief structure is generated through direct removal of the optical material in a controlled manner without any intermediate processes. Replication techniques generate copies of surface relief structures in polymers or other materials from a “master” element. The choice of fabrication method is generally driven by two main factors: function and cost. Each method has various advantages and disadvantages. In many cases, the required performance of the DOE will inherently limit the fabrication methods that can be used. Photolithographic processing of diffractive optics using binary masks will be employed as the primary model for the discussion on fabrication in this text. A survey of other fabrication methods is presented in Chapter 8.

## 6.2 Photolithography: A Method for DOE Fabrication

In general, the most common processes for fabrication of diffractive optical elements involve photolithographic methods that borrow heavily from the microelectronics industry. They are based on the same processes used to fabricate integrated circuits.<sup>2–5</sup> Because the size of the features and the need for flexibility of pattern generation are similar to those in manufacturing semiconductor devices, lithographic methods are optimal for many types of DOE fabrication. These methods are based on the use of photoresist, a light-sensitive conformal polymer. A simpli-

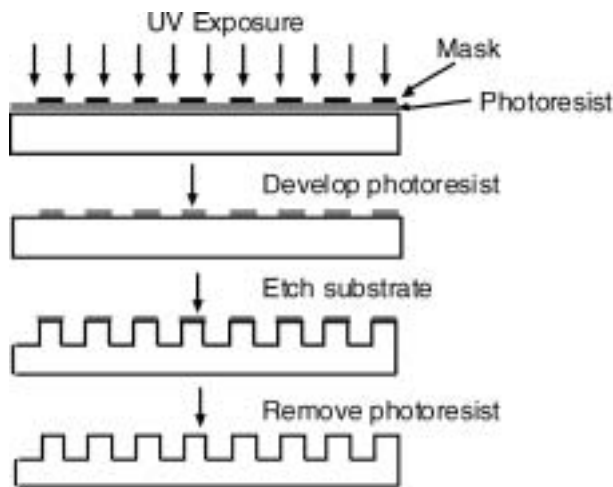


**Figure 6.2** Photolithographic processing and etching.

fied version of the photolithographic processing sequence followed by an etching step is shown in Fig. 6.2. A more elaborate one will be presented in Chapter 7.

The next few chapters will focus on various aspects of lithographic fabrication and testing. A specific approach that generates up to  $2^N$  phase levels from  $N$  binary transmission masks (commonly referred to as the *binary optics* method) will be used as an example throughout these chapters. We will examine issues related to mask generation, substrate testing, facilities, photoresist processing, etching into substrates, and DOE testing in detail.

### 6.3 From Equation to Component

Once the appropriate optical phase function is determined from the design process (discussed in earlier chapters), it is necessary to “translate” this phase function into a geometric surface relief pattern. In the scalar “thin-phase” approximation used for most diffractive optics, the surface profile can be split into two independent parts:

1. The lateral transition points in the pattern, which correspond to changes in the phase profile by  $2\pi$  or some appropriate fraction of  $2\pi$ .
2. The depth of the diffractive phase structure, which is determined by the wavelength of the incident light and the refractive indices of the substrate and surrounding material.

#### 6.3.1 Converting function to form

As noted earlier, the geometry of the surface structure determines the function of the DOE. In some cases this can be represented by a relatively simple equation,

while more complex DOEs must be designed numerically and iteratively on a computer, as discussed in previous chapters. As a simple example, consider the phase grating shown in Fig. 6.1. The period  $\Lambda$  of the grating determines the diffraction angles of the resulting diffraction orders, as given by the grating equation:

$$m\lambda = \Lambda(\sin \theta_m - \sin \theta_i), \quad (6.1)$$

where  $\lambda$  is the wavelength of the incident light,  $\theta_i$  is the angle of the incident light wave, and  $\theta_m$  is the diffraction angle of the  $m$ th diffraction order. Both  $\theta_i$  and  $\theta_m$  are measured from the normal to the grating plane, not the grating facets. Similarly, the relative phase difference imparted to the incident light wave is directly proportional to the depth of the local surface relief structure. The relationship between phase and depth is given by

$$d(x, y) = \frac{\phi(x, y)}{2\pi} \frac{\lambda}{(n_1 - n_0)}, \quad (6.2a)$$

for a transmissive DOE. For a reflective DOE, the depth is

$$d(x, y) = \frac{\phi(x, y)}{2\pi} \frac{\lambda}{2n_0}, \quad (6.2b)$$

where  $\phi(x, y)$  is the phase in radians, and  $n_1$  and  $n_0$  are the indices of refraction of the substrate material and the surrounding medium at the operating wavelength, respectively. These simple equations “translate” the requirements for many diffractive optical elements from an optical function into a tangible design. We now consider a simple example.

### 6.3.2 Example: 1 × 2 beamsplitter

Consider the example of a transmissive binary phase grating designed to operate as a 1 × 2 splitter with an He:Ne laser ( $\lambda = 0.6328 \mu\text{m}$ ) with an angle of 18.2 deg between the +1 and −1 diffraction orders. Using the grating equation with normally incident light, the period  $\Lambda$  of the grating is determined to be 4.0  $\mu\text{m}$ . Because the duty cycle of the grating is 50%, the width of the feature  $b$  in such a grating is 2.0  $\mu\text{m}$ . If the incident medium is air, and the substrate material is fused silica ( $n = 1.4572$  at 0.6328  $\mu\text{m}$ ), then the depth of the structure is [Eq. (6.2)]

$$d = \frac{\pi}{2\pi} \frac{0.6328\mu\text{m}}{(1.4572 - 1)} = 0.6920\mu\text{m}. \quad (6.3)$$

A scanning electron microscope (SEM) image of this grating is shown in Fig. 6.3. Equations (6.1) and (6.2) also apply to more complex beam fanouts. The period of the grating structure determines the angular separation between the diffraction orders, while the structure *within* a single grating period determines how the power is distributed between the orders. Even in more complex cases, the depth of the grating is determined only by the incident wavelength and the indices of refraction.

# Chapter 7

## Photolithographic Fabrication of Diffractive Optical Elements

### 7.1 Photolithographic Processing

The photolithographic processes used for fabrication of diffractive optical elements adapted from the microelectronics industry were broadly described in the previous chapter. These methods are based on the use of photoresist. A more detailed photoresist processing sequence is shown in Fig. 7.1. In this chapter we examine the principles of photolithography and etching and explore their application to the fabrication of diffractive optical elements using binary lithographic masks. Additional

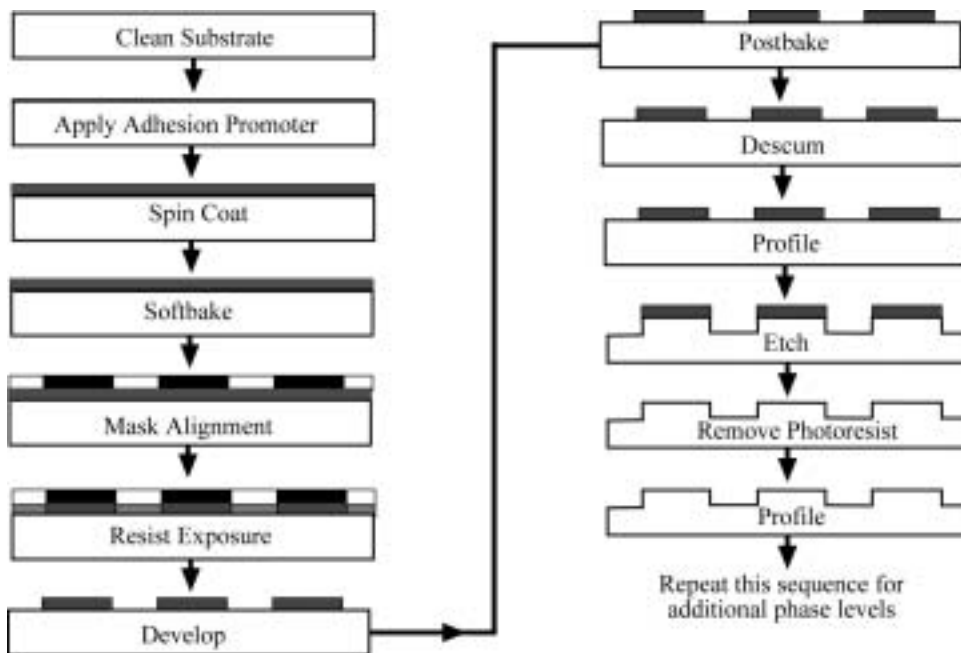


Figure 7.1 Photoresist processes for fabrication of diffractive optical elements.



information on the principles of photolithography can be found in a number of texts.<sup>1-7</sup>

### 7.1.1 Photoresist coatings

As indicated, photolithographic methods are based on the use of photoresist to create relief structures on substrate surfaces. This structure is used as a masking material to protect the underlying substrate during subsequent processing steps. In some cases, the photoresist structures themselves can be used as diffractive optical elements. Photoresists can be either positive, where the exposed resist dissolves upon development, or they can be negative, where the exposed resist polymerizes and remains after development. Positive photoresists are the most common type and are used in the processing examples given in this text.

There are many types of photoresists, each of which has been optimized for different applications. Most photoresists consist of three main chemical constituents: the photoactive compound (PAC), the solvent carrier, and the matrix material in which the PAC and solvent are contained. The PAC is the “light-sensitive” component of the photoresist and is typically designed to give optimal response at a specific exposure wavelength. The PAC in positive resists is typically diazide naphthaquinone, or DNQ. The solvent keeps the resist in a liquid state during storage and initial processing steps. The matrix material (usually a novolak resin) gives the photoresist its mechanical properties and serves as the protective layer after exposure and development. The reaction to incident light determines the quality of the three-dimensional photoresist pattern created from the two-dimensional lithographic mask. Different resists respond differently to different exposure wavelengths. This behavior can be quantified through three response parameters (A, B, C), referred to as the *Dill parameters* after a pioneer in the field of lithography modeling. The Dill parameters are defined as follows:

- *Absorption parameter A* ( $1/\mu\text{m}$ ): This describes the bleachable absorption of the resist. A positive value means the resist bleaches (positive resist) and a negative value implies that the resist darkens. This is the absorption of the photoresist before exposure.
- *Absorption parameter B* ( $1/\mu\text{m}$ ): This gives the absorption after the photoresist has been exposed and bleached. This is the nonbleachable part of the resist absorption. The thicker the layer of the photoresist and the larger parameter B is, the less light will reach the layers closer to the substrate surface.
- *Rate constant C* ( $\text{cm}^2/\text{mJ}$ ): This parameter describes how fast the photoresist is exposed.

Graphs of the A and B Dill parameters for a positive photoresist are shown in Fig. 7.2.

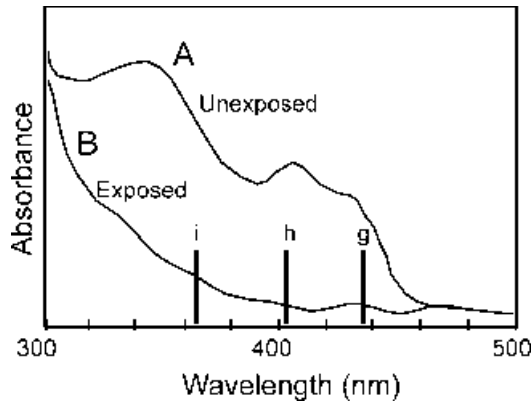


**Figure 7.2** Sample graph showing absorbance properties for exposed and unexposed photoresist.

### 7.1.2 Spin coating photoresist

After a substrate is cleaned, the first step of the photolithographic process is coating the substrate with a thin (typically microns or less) layer of photoresist. Thin, uniform coatings of photoresist are generated by spin coating the wafer. In many cases, adhesion promoters such as hexamethyldisilazane (HMDS) are applied to the clean wafer surface before spin coating to improve the adhesion of the photoresist layer to the substrate. During spin coating, liquid photoresist is dispensed on a substrate as it rotates at high rates (typically thousands of revolutions per minute). As the liquid resist spreads across the surface, the solvents in the resist begin to evaporate, causing the photoresist to slightly harden so that a skin begins to form on top (Fig. 7.3).

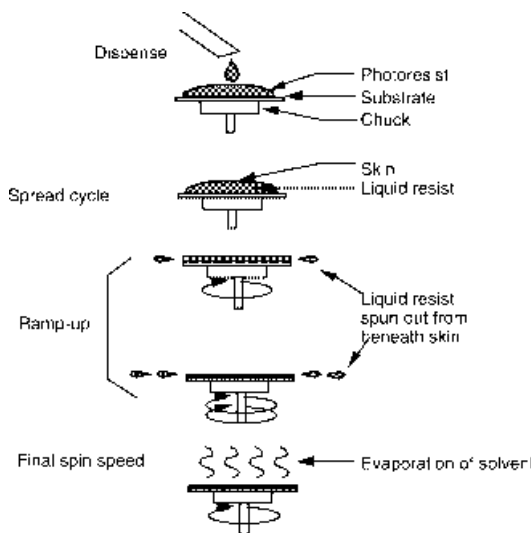


**Figure 7.3** Spin coating photoresist onto substrates.